1
2

Counting giraffes: A comparison of abundance estimators on the Ongava Game Reserve, Namibia

3

Christophe Bonenfant[1], Ken Stratford[2], and Stéphanie Périquet[2]

4
5
6
7
8
9
10
11

[1]*(Corresponding author, orcid.org/0000-0002-9924-419X) Université de Lyon, F-69000, Lyon ; Université Lyon 1 ; CNRS, UMR 5558, Laboratoire de Biométrie et Biologie Évolutive, F-69622, Villeurbanne, France. E-mail: christophe.bonenfant@univ-lyon1.fr*
[2]*Ongava Research Centre, Private Bag 12041, Ausspannplatz, Windhoek 9000, Namibia. orcid.org/0000-0001-7585-982X*
[2]*Ongava Research Centre, Private Bag 12041, Ausspannplatz, Windhoek 9000, Namibia. orcid.org/0000-0001-8901-3729*

12

Running title: Population size estimator for giraffes

Abstract

Camera-traps are a versatile and widely adopted tool for collecting biological data for wildlife conservation and management. While estimating population abundance from camera-trap data is the primarily goal of many projects, the question of which population estimator is suitable for analysing these data needs to be investigated. We took advantage of a 21 day camera-trap monitoring period of giraffes (*Giraffa camelopardalis angolensis*) on the Ongava Game Reserve (Namibia) to compare capture-recapture (CR), rarefaction curves and *N*-mixture estimators of population abundance. A marked variation in detection probability of giraffes was observed both in time and between individuals, with a skewed occurrence of animals at some waterholes. The mean daily visit frequency of waterholes by giraffes was $f = 0.25$ although they were less likely to be detected after they were seen at a waterhole. We estimated the population size to be 104 giraffes ($C_v = 0.02$) using the most robust reference estimator (CR). All other estimators deviated from the CR population size by *ca.* -16 to $> +106\%$. This was due the fact that these models did not account for the temporal and individual variations in detection probability. We found that modelling choice was much less forgiving for *N*-mixture models than CR estimators because the former leads to very variable and inconsistent estimations of abundance. Double counts were problematic for *N*-mixture models, challenging the use of raw counts (*i.e.* when individuals are not identified), to monitor the abundance of giraffe or of other species without idiosyncratic coat patterns.

Keywords:
camera trap
Giraffa camelopardalis
large mammal
multiple counts
population size
savannah

Introduction

The on-going development and large-scale deployment of camera trapping technology offers a promising and appealing way for ecologists to collect a variety of biological data at an unprecedented scale and speed (Swanson et al. 2015). Habitat use, activity patterns and population abundance are now frequently studied using camera trap data (O'Connell et al. 2011; Trolliet et al. 2014). Sampling a population with camera-traps is indeed particularly useful and efficient (Wearn & Glover-Kapfer 2019), even more so for species with idiosyncratic coat patterns from which individual identification is possible (*e.g.* Jackson et al. (2006); Karanth & Nichols (1998); Stratford & Stratford (2011)). Camera trap data are increasingly used to estimate population abundance (Burton et al. 2015; Gilbert et al. 2021) but such data come with specific problems. Detection rate is not perfect, and sampling design and effort are likely different from physical captures (Hamel et al. 2013; Gilbert et al. 2021). While obtaining unbiased estimates of abundance is of central importance for conservation and wildlife management to set appropriate goals and policies (Anderson 2001), the suitability of the currently available population abundance estimators for camera-trap data remains to be evaluated empirically.

For populations living in the wild, the main issue is of an underestimation of abundance because an unknown proportion of animals are missed during surveys, *i.e.* animal detection is not perfect (Strandgaard 1967; Apollonio et al. 2010). Imperfect detection is the main reason why detection probability of individuals

underpins most population abundance estimators (Seber 1982; Schwarz & Seber 1999). Past empirical studies showed how detection probability can vary in both time and space (Otis et al. 1978). For instance, detection probability was reported to increase with habitat openness (Choquenot 1995), vary between con-specifics with different behavioural repertoires (*i.e.* personalities, see Le Cœur et al. 2015, for an example on Siberian chipmunk *Tamias sibiricus*), decrease with the distance of animals from the observer (Burnham et al. 1980; Buckland et al. 2000), between observers themselves depending on their experience or motivation in spotting animals (Collier et al. 2007; Zett et al. 2022), and between camera trap brands or orientation (Rovero et al. 2013).

Accounting for these intrinsic and extrinsic sources of detection heterogeneity has profound consequences for the accuracy and precision of population abundance estimations (Veech et al. 2016). Currently, only a handful of population abundance estimators can account for the multiple sources of variability in detection probability, and most derive from either distance sampling (DS) and capture-recapture (CR). Both families of estimators can accommodate detection rate for known sources of variability like time of the year, habitat type, or sex and age of individuals (Pollock 1980; Schwarz & Seber 1999). However, only the CR approach can model unmeasured or unknown sources of heterogeneity. The reason why these two methods are not systematically implemented in the field is due to serious practical limitations. CR requires a substantial proportion of the population to be recognizable: for instance Strandgaard (1972) recommended that up to 2/3 of a roe deer (*Capreolus capreolus*) population should be marked to

91 obtain robust results. In addition, the capture and marking of wild animals can

92 raise ethical questions for endangered species. DS on the other hand, is quite

93 sensitive to the sampling design (*e.g.* linear transects and coverage), and is

94 sometimes difficult to carry out in dense tropical forests of Africa (Duckworth

95 1998), or when human disturbance induces behavioural responses (see Elenga et

96 al. 2020, on blue duikers *Philantomba monticola*). In other words, these two

97 reference methods for estimating animal abundance can rapidly become

98 prohibitively expensive, time consuming and difficult to implement at large spatial

99 scale for wildlife managers (Morellet et al. 2007).

100 By seeking to keep implementation costs low, practitioners often make use of

101 easier-to-implement, cheaper methods to monitor wildlife populations at spatial

102 scales compatible with wildlife management (Morellet et al. 2007). This choice

103 often comes at the costs of using estimators with less flexibility in accounting for

104 variability in detection rate. For instance, catch-per-unit effort (Leslie & Davis

105 1939) or rarefaction curves (Petit & Valiere 2006) can return an estimate of`

106 population size from unmarked animals, but both assume constant detection rates

107 for all individuals over the sampling period. A noticeable exception is the *N*-

108 mixture model (Royle 2004), which allows the separation of population size from

109 detection probability using repeated counts of animals in time and space. The

110 robustness and accuracy of *N*-mixture abundance estimators is, however,

111 frequently questioned (Kéry 2018).

112 For decades in large African national parks, a common practice has been to

113 monitor wildlife using indices of population abundance of large herbivore species

114 **5**

115   from direct (observation of animals) or indirect observations (observation of signs

116   like tracks, faeces) (Jachmann 2002; 2012). Such indices can be obtained through

117   road transects counts (with visibility issues), aerial counts (with visibility issues and

118   high costs), and waterhole counts of various duration (with the risk of missing

119   water-independent species). The underlying assumption of a constant detection

120   rate has been advanced to be the main reason for indices of population

121   abundance to fail at monitoring wildlife abundance reliably (Anderson 2001).

122   However, these indices might be suitable for use by managers following a

123   validation test against a reference method (Morellet et al. 2007). While several

124   studies show that not accounting for detection variability can indeed bias

125   population abundance estimates (Dail & Madsen 2011), the magnitude and

126   direction of this bias is seldom quantified empirically.

127   The giraffe (*Giraffa camelopardalis ssp.*) is a charismatic species of

128   conservation significance with decreasing populations in many parts of Africa

129   (O'connor et al. 2019). The assessment of local populations' conservation status

130   and their long-term viability are however hampered by the many different ways

131   abundance has been estimated between study areas. Here, we propose to take

132   advantage of waterhole monitoring with camera traps on the Ongava Game

133   Reserve, Namibia, to compare six population size estimators to characterize the

134   biases associated with spatial, temporal and individual variability in detection

135   rates. Being water dependent but with a capacity to spend several days without

136   drinking, individual giraffes typically come to drink every two or three days

137   (Shorrocks 2016). This behaviour can potentially generate variation in detection

138   **6**

probability once individuals have visited a waterhole, *i.e.* an individual seen on a given day will be less likely to be seen on the following day. It is also known that males and females have different behaviours and resource requirements (see Gaillard et al. 2003, for examples in different large herbivore species), therefore the frequency of waterhole visit might differ between sexes (Shorrocks 2016).

A practical advantage of using giraffe as a study species is that one can use its idiosyncratic coat patterns to uniquely identify individuals from photographs, and then apply CR estimators to evaluate population abundance (Brown et al. 2019; Lee et al. 2022). This biological feature offers the opportunity to quantify the impact of detection heterogeneity on population size estimates, and to assess the relevance of simpler indices of abundance to monitor giraffe (and other species) populations. We compared the abundance estimates obtained from proven CR methodologies, with *N*-mixture estimates, rarefaction curves, and raw count data (by observers) on the Ongava Game Reserve in 2016.

Material and Methods

Study area

Ongava Game Reserve (OGR) is located in Namibia, covering an area of approximately 300km^2 immediately to the south of Etosha National Park with a common boundary on Ongava's north side (Fig. 1). OGR is enclosed by electrified fences preventing movement of ungulates in and out the reserve. OGR hosts several large mammalian predators including lion (*Panthera leo*), cheetah

161   (*Acynonyx jubatus*), leopard (*Panthera pardus*) and spotted hyena (*Crocuta*

162   *crocuta*), all potential predators of juvenile or adult giraffes (Shorrocks 2016).

163   Hunting is prohibited on OGR and poaching of giraffes is unlikely due to a high-

164   intensity anti-poaching presence on the reserve.

165   The habitat is termed *Karstveld*, with vegetation primarily (*Colophospermum*

166   *mopane*) shrub and woodland, with some areas savannah-like. OGR's relief is

167   mostly dolomite hills, with a few small open plain areas and a well-defined ridge

168   and small mountains in the central and northern part of the reserve. The weather

169   zone for the reserve is typical for semi-arid northern Namibia, with an average

170   annual rainfall of 380mm (see Stratford & Stratford 2011, for further details).

171   There are several natural dams on the reserve, although most of these only

172   contain water during the rainy season (January - April). During the dry season

173   (May to December) water is only available at 12 artificial waterholes.

174   Count data

175   From the 8th to the 28th of September 2016 (a total of 21 days), between three and

176   eight camera traps (®Reconyx RC-55 and HC-500 and ®Bushnell Trophy series)

177   were deployed at each waterhole to monitor their usage by wildlife (see Table S1).

178   Each camera was mounted inside a stainless-steel protection case bolted to a tree

179   or a pole within 10–15m of the waterhole. Reconyx cameras were set to record a

180   sequence of 10 images with a delay of 30 seconds between sequences, while

181   Bushnell cameras recorded sequences of 3 images with a delay of 15 seconds. We

182

183   extracted all images containing giraffe and their associated metadata (date and

184   time).

185   The camera traps yielded a total of 30 913 giraffe images. From these, 85 were

186   discarded because the date and time of capture recorded by the camera were

187   wrong. When possible, individual giraffe were manually identified in each image

188   based on their unique coat patterns with the help of HotSpotter software (Crall et

189   al. 2013). Whenever a giraffe could not be identified from its coat patterns or with

190   the help of other images in the sequence, it was labelled as unknown. Where

191   possible, we recorded the age-class (adults, sub-adults and juveniles) and sex of

192   each individual.

193   Population size estimations

194   *Capture-Recapture models*

195   We built daily capture histories for each individual giraffe over the t = 21 days of

196   the camera trap survey. We then analysed these capture histories with CR

197   methods (Lebreton et al. 1992) in a Bayesian framework (see Kéry & Schaub

198   2011). Each giraffe observation at a waterhole is the product of survival (ϕ) and

199   detection (p) probabilities, conditional on first observation. We implemented

200   closed population estimators of abundance because of the fence running all

201   around OGR, and because preliminary analyses estimated survival rate to ϕ = 1

202   from open population models. We modelled detection probability p on the logit

203   scale as a function of time (*i.e* day, categorical variable with 20 levels), whether

204   **9**

205   the individual was seen at any waterhole the previous day or not (categorical

206   variable with 2 levels), and of the total number of functioning cameras

207   (covariate). We also included random effects of the individual (σ^2_{id}) and of time

208   (σ^2_t). Because we could not identify the sex of two individuals, we treated sex as a

209   latent Bernouilli variable S_i of parameter π corresponding to the population sex-

210   ratio. We then entered S_i as an explanatory variable (categorical variable with 2

211   levels) of *p*. Taken together, our set of fitted models covered the standard

212   estimators for population size namely M_t (time effect), M_{th} (time and individual

213   heterogeneity effects) and M_{tbh} (time, individual heterogeneity and behavioural

214   effects: see Otis et al. 1978). In addition to these standard models, we fitted a

215   spatially explicit model (SECR, Efford 2004) to estimate giraffe population size

216   using the the SCRBayes R package (Royle et al. 2009), hence accounting for

217   movement of animals between waterholes. We selected the statistically significant

218   variables from the posterior parameter distributions and only kept variables for

219   which 0 was excluded from the 95% credible interval.

220   *Rarefaction curves*

221   We also estimated population size using the rarefaction curves method (see Petit

222   & Valiere 2006). Rarefaction curves have been used for decades to estimate`

223   species diversity (Colwell & Coddington 1994). Over the course of the survey, the

224   cumulative number of different giraffe seen at waterholes (hereafter noted C_t)

225   **10**

226   increased from day 1 to day 21 (see Fig. 2). Two different non-linear functions

227   have been proposed in the literature for the case of population size estimation:

228   1. the hyperbolic function (Kohn et al. 1999): $C_t = (N_s \times t)/(b - t)$;
229   2. the exponential function (Eggert et al. 2003): $C_t = N_s \times (1 - e^{-c \times t})$;

230   where t is time in days ranging from 1 to 20, and b and c are breakage

231   parameters, *i.e.* the rate of decrease of the number of new individuals adding up

232   in time. We therefore fitted the two functions to the cumulative number of new

233   giraffe C_t in a Bayesian model to produce another estimate of population size (N_s).

234   Note that this approach assumes a constant detection rate over time, space and

235   between individuals, given by $p_s = C_{21}/N_s$ and requires individuals to be uniquely

236   identified. We assessed the fit of the data to these models with a χ^2 goodness-of-

237   fit (GOF) test. We hence compared the sum of the difference between fitted and

238   expected numbers of giraffes seen per day, each squared and divided by the

239   expected value, to a χ^2 with $t - 3$ degrees of freedom (two model parameters + 1)

240   at a significance level $\alpha = 0.05$.

241   *N-mixture models*

242   The third population size estimator we applied was the *N*-mixture model (Royle

243   2004). The *N*-mixture model assumes that repeated counts of animals in time and

244   space are the outcome of combined probability models for the unknown

245   population abundance (N_N) and for the detection (p_N). For population abundance,

246   the Poisson, negative binomial and zero-inflated Poisson distributions are the

247   **11**

248 most commonly used, but other discrete distributions may be considered (see

249 below). For the detection process, a binomial distribution (with parameters N_N and

250 p_N) accounts for undetected animals. The *N*-mixture model assumes a

251 demographically closed population and an equal detection probability for all

252 individuals. We estimated population size by fitting four *N*-mixture models to the

253 giraffe data (t = 20 days, s = 12 waterholes), allowing for temporal variation in

254 detection probabilities (Kéry et al. 2009).

255   We replicated the analyses of population size estimation for two data sets. The

256 first data set consisted in the number of different and uniquely recognized giraffe

257 seen per day at each of the 12 waterholes. We used a binomial distribution to

258 model the observation process. Here, we considered another distribution mixture

259 accounting for the non-independence between individuals, the β-binomial–

260 binomial *N*-mixture models (Martin et al. 2011). We discarded the zero inflated

261 Poisson – binomial mixture because of its poor performance in general (Veech et

262 al. 2016). For the second data set, we used the total number of giraffe seen

263 (without individual recognition) and was hence more closely related to counts

264 carried out in many reserves where individuals identification is not done. Here, we

265 used a Poisson model for the observation process because double counts were

266 very frequent from camera-trap photographs, resulting in a Poisson–Poisson

267 distribution mixture (Kéry & Royle 2020). To achieve convergence and facilitate

268 parameter estimations, we included a temporal correlation for detection rates

269 (first order autoregressive model, see Kéry & Royle 2020, p. 305–306). Note that in

270   **12**

271　the case of Poisson – Poisson N-mixture models, we no longer estimate a

272　detection probability ($0 < p < 1$) but a detection rate instead ($\psi > 0$).

273　　　　We fitted all CR (except SECR), rarefaction and N-mixture models using

274　JAGS 4.0 (Plummer et al. 2003). We used non-informative prior distributions for all

275　estimated parameters except for N_s in the rarefaction curves models, for which we

276　used a half-normal distribution to ensure that number of animals was > 0. We ran

277　three Monte-Carlo (MCMC) chains, with a burn-in of 10000 iterations before saving

278　5000 iterations to get the posterior distributions of parameters at convergence. We

279　checked convergence graphically to ensure good mixing of MCMC chains and used

280　Gelman's h for an objective convergence criterion (convergence is reached when h

281　is close to 1 Gelman & Pardoe 2006). The R and JAGS code we used is freely

282　accessible on-line at https://github.com/cbonenfant.

283　**Results**

284　Camera trap data set

285　Giraffe were recorded at 10 of the 12 waterholes surveyed. A total of 101

286　individuals were identified from the camera trap images: 58 adult females, 41

287　adult males and two juvenile of unknown sex. For all but six individuals, we

288　obtained identification images from both sides of the animal. For five individuals,

289　we only had images from the left side and only a front shot for the remaining

290　animal. The majority of individuals (66%, $n = 58$) were seen at a single waterhole,

291　while 27% ($n = 24$) and 7% ($n = 6$) were seen at two and three waterholes

292　　　　　　　　　　　　　　　　　　　　　　　　　　　　　　**13**

293 respectively. On average, 28 unique giraffes were detected per day with camera

294 traps, with a minimum of 8 and a maximum of 54 (median of 29.5 individuals). For

295 98% of the individuals, we could assign the age-class.

296 Population size estimates

297 *Capture-recapture models*

298 From capture histories, the best model describing the observed variability in

299 detection rate included time variation (*i.e.* differences in detection probability

300 between days), sex ($\hat{\beta}$ = $_{-0.60}$ −0.14 $_{0.30}$), whether the individual was seen at any

301 waterhole the day before ($\hat{\beta}$ = $_{-2.95}$ −2.32 $_{-1.74}$), and the first order interaction

302 between sex and previous visit ($\hat{\beta}$ = $_{0.41}$ 1.17 $_{1.93}$). We detected a marked variability

303 in daily detection probabilities over the course the of the study, ranging from $\hat{p}$ =

304 $_{0.00}$ 0.02 $_{0.05}$ on day 1, to $\hat{p}$ = $_{0.35}$ 0.47 $_{0.59}$ on day 15. On any day, females were $_{0.03}$

305 0.11 $_{0.18}$ times less likely to be detected at any waterhole

306 following a detection, while a male was $_{0.15}$ 0.30 $_{0.50}$ times less likely to be detected

307 if it was seen the day before. Once time, sex and previous visit had been

308 accounted for, the remaining individual heterogeneity in detection rate was ($\hat{\sigma}^2_{id}$ =

309 $_{0.40}$ 0.71 $_{1.21}$). The population size estimate returned from our best model of

310 detection rate was $\hat{N}$ = $_{101}$ 104 $_{109}$ individuals (Table 1). Using SECR to account for

311 animal movement and the spatial distribution of camera traps on

312 OGR increased the population size by 5%, with an estimate of $\hat{N}$ = $_{103}$ 109 $_{115}$.

313 Parameter estimates for the SECR models were $\hat{\sigma}$ = $_{1868.92}$ 1981.20 $_{2102.03}$ for scale

314 **14**

315   of the half-normal distribution, corresponding to the average movement radius of

316   giraffes, and $\hat{\lambda}_0 = {}_{0.24}\,0.28\,{}_{0.32}$ for the expected detection rate of an individual

317   whose home-range centre is exactly at the trap location.

318   *Rarefaction curve models*

319   We calculated the cumulative number of newly detected individuals over the 20

320   days duration of the study (Fig. 2). The number of new individuals increased

321   steeply up from day 1 to day 16 when it started to level off. It took 19 days to

322   observe all the individuals identified during the study period (Fig. 2). Fitting the

323   hyperbolic and exponential rarefaction curves to estimate population size gave

324   contrasting results (Table 1). While the exponential equation returned a

325   population size of ${}_{104}\,117\,{}_{134}$ giraffe, the hyperbolic equation projected a

326   population size 49% larger (${}_{145}\,175\,{}_{215}$). Breakage coefficients were $\hat{b} = {}_{0.09}\,0.12\,{}_{0.16}$

327   and $\hat{c} = {}_{7.9}\,11.9\,{}_{17.7}$ for the exponential and hyperbolic equations respectively.

328   Overall, the fit of the two rarefaction curves to the data was poor for the

329   exponential and hyperbolic equations (Fig. 2), with $\chi^2_{df=18} = 339.4$ and $\chi^2_{df=18} =$

330   330.1, both GOF tests rejected the null ($\chi^2_{df=18} = 9.39$ at the confidence level $\alpha =$

331   0.05). Precision of the estimates was of the same magnitude, close to 10% for

332   both models (Table 1).

333   *N-mixture models*

334   We applied three different *N*-mixture models yielding contrasting results. The

335   **15**

336   Poisson–binomial model returned an estimate of $\widehat{N}_{PB}$ = $_{173}$ 215 $_{263}$ giraffes (Table 1),

337   hence 80% larger than the estimation from the best CR model. The β-binomial –

338   binomial mixture estimated abundance to $\widehat{N}_{\beta BB}$ = $_{107}$ 124 $_{156}$ giraffes. The associated

339   parameters of the β-binomial function were

340    $\hat{\alpha}$ = $_{0.32}$ 0.44 $_{0.58}$ and $\hat{\beta}$ = $_{1.13}$ 1.82 $_{2.91}$, giving a correlation $\hat{\rho}$ = $_{0.22}$ 0.31 $_{0.40}$. According

341   to this model, the mean daily detection probability was $\hat{p}$ = $_{0.14}$ 0.20 $_{0.25}$, ranging

342   between $\hat{p}$ = $_{0.00}$ 0.01 $_{0.10}$ and $\hat{p}$ = $_{0.63}$ 0.87 $_{0.99}$. Fitting a Poisson–Poisson N-mixture

343   model to raw observations led to an estimated population size of $\widehat{N}_{PP}$ = $_{79}$ 87 $_{99}$

344   giraffe (Table 1). The mean detection rate was $\hat{\psi}$ = 0.55 but varied from $\hat{\psi}_{k,t}$ = $_{0.00}$

345   0.01 $_{0.03}$ to $\hat{\psi}_{k,t}$ = $_{1.79}$ 3.11 $_{5.10}$ according to time and space. The first order temporal

346   auto-correlation coefficient (AR(1)) was estimated as $\hat{\tau}$ = $_{-1.00}$ −0.56 $_{-0.03}$. Note that

347   the Poisson-Poisson model was particularly difficult to fit to the data as we

348   experienced many convergence

349   issues.

350   Frequency of waterhole visits

351   We computed the mean time of return to a waterhole and frequency of visits from

352   the daily probabilities as estimated from the CR model. To do so, we simulated 5

353   000 capture histories from a multinomial distribution taking the observed

354   detection probabilities for each day as the distribution model parameters. For

355   each capture history, we calculated the difference in days between successive

356   visits to any waterhole, and its inverse to get the frequency of visits. The mean

357   **16**

358   time of return to a waterhole of giraffe was $\hat{T}_l =$ $_{1.6}$ 5.0 $_{14.0}$ days for males, yielding a

359   frequency of $\hat{f} =$ $_{0.07}$ 0.26 $_{0.62}$. Females tended to visit waterholes more frequently

360   with a mean time lag of $\hat{T}_l =$ $_{1.7}$ 4.0 $_{9.5}$ days between two observations, and a

361   frequency $\hat{f} =$ $_{0.10}$ 0.30 $_{0.58}$ over 20 days of monitoring.

Discussion

363   Population abundance is the core state variable of population dynamics from

364   which the population growth rates are derived (Caughley 1977). Our study system

365   at OGR offers a unique opportunity to apply and compare different methods to

366   estimating giraffe abundance. Because giraffe can be recognized from their coat

367   patterns, we were able to apply methods based on the re-observations of

368   individuals (capture-recapture *sensu largo*), which were then compared to other

369   abundance estimators traditionally used in wildlife monitoring in African national

370   parks (Jachmann 2012). With the exception of the Poisson-binomial *N*-mixture

371   model, all estimators yielded potentially acceptable results (see Table 1). In

372   comparison to the CR estimate, the other abundance estimators deviated by −16

373   to +106%. We caution against over-estimating giraffe abundance when using *N*-

374   mixture models or rarefaction curves at large scale and for conservation purposes.

375   As there is marked heterogeneity in detection probability in time and among

376   individuals, the drinking behaviour of giraffe likely accounts for the discrepancies

377   we report among abundance estimators, and should be carefully considered for

378   other species monitored at waterholes.

17

380   Individual variability, local habitats and the use of a plethora of available

381   methods to estimate population abundance (Seber 1982) have led to inconsistent

382   ways of monitoring wild populations of large herbivores among and, sometimes,

383   within sites. For instance, in Hwange National Park, Zimbabwe, giraffe density

384   estimation was derived from distance sampling (Valeix et al. 2008), while in the

385   Serengeti, Kenya, aerial counts were preferred as an index of abundance (Strauss

386   2014, see also Table 1 for an overview). We show here that the choice of a

387   particular method to estimate giraffe abundance has profound consequences on

388   the results. On OGR, the range of estimated population sizes varied by more than

389   two-fold, from 87 to 215, yielding densities of 0.29 and 0.71 individuals.km^{-2}.

390   Which estimator to implement and to apply to empirical data is not trivial, and

391   comparisons of results with well-known, reference methods is advised (*e.g.*

392   Corlatti et al. 2017; Pellerin et al. 2017). In our case, and in the absence of

393   knowledge of the true number of giraffes, we considered the population size of

394   104 giraffes (density of 0.34 individuals.km^{-2}) derived from CR models to be the

395   most reliable among all estimates. CR methods are usually regarded as the gold

396   standard because of their flexibility in dealing with detection probability and the

397   long history of use since the publication of its principle by Petersen-Lincoln

398   (Pollock 1976).

399   While population size as estimated from Eggert's equation is somewhat close

400   to CR models (117 vs. 104), the estimation from Kohn's equation seems

401   biologically unrealistic and should be disregarded (see also Frantz & Roper 2006,

402   **18**

403   for similar results on simulated data). With 175 individuals, giraffe density (0.58

404   individuals.km^{-2}) would be almost 3 times larger than previous estimates at Etosha

405   National Park (Table 2), neighbouring OGR with similar rainfall conditions (Fig. 1).

406   Such a high population density should trigger density-dependent processes, first

407   manifested by a reduction in reproduction rates of females or low juvenile survival

408   in large herbivores (Bonenfant et al. 2009). Rarefaction curves were shown to give

409   biased estimation of biodiversity when species are not uniformly distributed in

410   space (Collins & Simberloff 2009). Similarly, projecting the number of total

411   individuals from rarefaction curves (*e.g.* Petit & Valiere 2006) is likely to be

412   influenced by heterogeneity in detection` probability among individuals. While

413   Kohn's equation returned a large number of giraffe compared to the CR estimate,

414   Eggert's equation almost matched our reference population size. However, with

415   no replication of our observations and counts, we cannot assess the robustness of

416   Eggert's equation to heterogeneity in detection probability among individuals. All

417   in all, the fit of the two rarefaction curves were poor (Fig. 2) making the inference

418   on population size spurious at best, in addition to requiring individual

419   identification of giraffes. If individual identification is to be done, we advise the

420   use of CR methods instead of rarefaction curves to estimate giraffe abundance.

421   Although *N*-mixture models are more and more used to analyse count data,

422   their reliability is regularly questioned (Dennis et al. 2015; Link et al. 2018; Knape

423   et al. 2018; Nakashima 2020). Comparisons with other proven methods such as CR

424   are scarce, despite their value. For giraffe, the estimation of population

425   **19**

426 abundance from *N*-mixture models suffers from either a severe overestimation

427 (215 for the Poisson–binomial) to an underestimation (87 for the Poisson–Poisson)

428 when applied on raw, unprocessed data without identification of individuals. If

429 individual identification is not possible, double counts are likely to occur in the raw

430 counts. Double counting therefore be a commonly encountered situation in count

431 operations at waterholes in many African parks. A Poisson-Poisson *N*-mixture is

432 the natural solution to this situation by estimating a detection rate ($\psi > 1$) where

433 individuals can be seen more than once. Unfortunately, our results suggest poor

434 performance of the Poisson–Poisson *N*-mixture model in estimating giraffe

435 abundance. This model produced the lowest population size estimate, being −36%

436 smaller than CR estimate (87 vs 119 giraffe). Despite the occurrence of frequent

437 double counts (empirical rate: 568/119 = 4.77 from CR data), the Poisson–Poisson

438 *N*-mixture model failed to estimate this quantity correctly ($\hat{\lambda} \times \hat{\psi} = 1.06$), maybe

439 because of unmodelled heterogeneity, in addition to temporal and spatial

440 variation in the detection probability of animals. Since most giraffe live in groups,

441 we also faced non-independence of individual detection which, when accounted

442 for with a β–binomial distribution in the *N*-mixture model (Martin et al. 2011),

443 returns much more sensible estimates of population size (124 individuals) than

444 any other assumed distributions of the detection process (Table 1).

445   A strength of CR estimators over the rarefaction curves and *N*-mixture models

446 is their ability to model detection probabilities not only in time and space, but also

447 at the individual level. An important source of heterogeneity in detection

448 probability we observed was the frequency of visit to waterholes. Giraffe visit to

449   **20**

450 waterholes is primarily motivated by thirst, and if they must drink on a regular

451 basis, they can skip drinking for several days in a row (Shorrocks 2016). On OGR,

452 giraffe's return frequency to waterholes was between 0.26 and 0.30 for males and

453 females respectively (one visit every 4–5 days on average), which is lower than

454 previously observed. For instance Shorrocks (2016) reported a frequency of 0.61,

455 while (Caister et al. 2003) recorded daily drinking in Niger ($f \approx 1$). Such a marked

456 difference in drinking frequency may have both biological and technical

457 explanations. On OGR, giraffes may find enough water in forage or access to small,

458 non-monitored water sources, making the need to visit larger but dangerous

459 waterholes less stringent. An alternative would be that camera traps might fail to

460 trigger in the presence of an animal, which is sensitive to camera placement,

461 settings and performance (Rovero et al. 2013; McIntyre et al. 2020), or because

462 the photograph was of too low quality to allow for individual identification (*e.g.*

463 blurry or dark images). Independently of its cause, this behaviour generates a

464 particular detection pattern. Once an animal has visited a waterhole to drink, it

465 will be less likely to be detected the following days, therefore breaking the

466 assumption of constant detectability of many abundance estimators. In CR

467 terminology, giraffe are "trap shy" and several solutions have been proposed by

468 statisticians to reduce bias on abundance estimates in the CR framework (Pollock

469 1980).

470   Our study on OGR is a clear illustration that the assumption of a constant

471 detection rate is not met, even with a fixed sampling design and a fine, daily,

472 temporal resolution of the monitoring. Detection probability varied substantially

473   **21**

from one day to another, ranging from 0.02 to 0.47. This result is a major warning

against the use of raw (*i.e.* unidentified individuals) count data, such as the

number of giraffes seen per day, to monitor giraffe populations in the wild (see

Anderson 2001, for a general argument). Variation in daily detection probability

resulted not only from the drinking and grouping behaviour of giraffe, but also

from the number of camera traps in service over the course of the study. Several

cameras stopped recording pictures because of battery failure or full memory

cards. A sampling design based on fixed camera traps at waterholes hence does

not guarantee a constant detectability. This marked variability in detection

probability in time likely accounts for the discrepancy we report among the six

population abundance estimators. In practice, estimating abundance of giraffe

should preferably consider methods flexible enough to account for their drinking

behaviour.

Sampling large mammal populations with camera traps is of great practical

advantage. When it comes to estimation of population abundance from camera-

trap data, the long-standing issues of detection and the modelling of its

heterogeneity in time, space and among individuals still apply. We found the

deviation of *N*-mixture and rarefaction curve models from our reference CR

estimation deteriorated when the data are not processed using individual

identification. For species with unique coat patterns, individual identification with

machine learning and artificial intelligence is now robust, efficient, and is

becoming more easily available and less of an obstacle for wildlife managers (see

Miele et al. 2021). This may apply to other African species of large herbivores such

498   as zebras sp., greater (*Tragelaphus strepsiceros*) and lesser kudu (*T. imberbis*),

499   wildebeest (*Connochaetes taurinus*) or bushbuck (*Tragelaphus scriptus*) that all

500   bear idiosyncratic marks. We believe the gain in precision in population

501   abundance estimation is worth the time allocated to it and will serve the

502   conservation of such species.

507   References

508 Anderson D.R., 2001. The need to get the basics right in wildlife field studies. Wildl.
509   Soc. Bull. 29:1294–1297.

510 Apollonio M., Putman R., Grignolio S., Bartoš L., 2010. Hunting seasons in relation to
511   biological breeding seasons and the implications for the control or regulation of
512   ungulate populations. In: Putman R., Apollonio M., Andersen R. (Eds.) Ungulate
513   Management in Europe, Cambridge University Press, 80–105.

514 Bonenfant C., Gaillard J.M., Coulson T., Festa-Bianchet M., Loison A., Garel M., Loe
515   L.E., Blanchard P., Pettorelli N., Owen-Smith N., Du Toit J., Duncan P., 2009.
516   Empirical evidence of density-dependence in popualtions of large herbivores. Adv.
517   Ecol. Res. 41:313–357.

518 Brand R., 2007. Evolutionary ecology of giraffes (*Giraffa camelopardalis*) in Etosha
519   National Park, Namibia. Ph.D. thesis, Newcastle University.

520 Brown M.B., Bolger D.T., Fennessy J., 2019. All the eggs in one basket: a countrywide
521   assessment of current and historical giraffe population distribution in Uganda.
522   Global Ecol. Conserv. 19:e00612.

523   **23**

524   Buckland S., Goudie I., Borchers D., 2000. Wildlife population assessment: past
525   developments and future directions. Biometrics 65:1–12.

526   Burnham K.P., Anderson D.R., Laake J.L., 1980. Estimation of density from line transect
527   sampling of biological populations. Wild. Monogr. (72):3–202.

528   Burton A.C., Neilson E., Moreira D., Ladle A., Steenweg R., Fisher J.T., Bayne E., Boutin
529   S., 2015. Wildlife camera trapping: a review and recommendations for linking
530   surveys to ecological processes. J. Appl. Ecol. 52(3):675–685.

531   Caister L.E., Shields W.M., Gosser A., 2003. Female tannin avoidance: a possible
532   explanation for habitat and dietary segregation of giraffes (*Giraffa camelopardalis*
533   *peralta*) in Niger. Afr. J. Ecol. 41(3):201–210.

534   Caughley G., 1977. Analysis of vertebrate populations. Wiley, London.

535   Choquenot D., 1995. Assessing visibility bias associated with helicopter counts of feral
536   pigs in Australia's semi-arid rangelands. Wildl. Res. 22(5):569–577.

537   Collier B.A., Ditchkoff S.S., Raglin J.B., Smith J.M., 2007. Detection probability and
538   sources of variation in white-tailed deer spotlight surveys. J. Wildl. Manag.
539   71(1):277–281.

540   Collins M.D., Simberloff D., 2009. Rarefaction and nonrandom spatial dispersion
541   patterns. Environ. Ecol. Stat. 16(1):89–103.

542   Colwell R.K., Coddington J.A., 1994. Estimating terrestrial biodiversity through
543   extrapolation. Philos. Trans. R. Soc. Lond., B, Biol. Sci. 345(1311):101–118.

544   Corlatti L., Nelli L., Bertolini M., Zibordi F., Pedrotti L., 2017. A comparison of four
545   different methods to estimate population size of Alpine marmot (*Marmota*
546   *marmota*). Hystrix 28(1):61–67.

547   Crall J.P., Stewart C.V., Berger-Wolf T.Y., Rubenstein D.I., Sundaresan S.R., 2013.
548   Hotspotter—patterned species instance recognition. In: 2013 IEEE workshop on
549   applications of computer vision (WACV), 230–237.

550   Dail D., Madsen L., 2011. Models for estimating abundance from repeated counts of
551   an open metapopulation. Biometrics 67(2):577–587.

552   Dennis E.B., Morgan B.J., Ridout M.S., 2015. Computational aspects of *N*-mixture
553   models. Biometrics 71(1):237–246.

554

555 Duckworth J., 1998. The difficulty of estimating population densities of nocturnal
556   forest mammals from transect counts of animals. J. Zool. 246(4):443–486.

557 Efford M., 2004. Density estimation in live-trapping studies. Oikos 106(3):598–610.

558 Eggert L., Eggert J., Woodruff D., 2003. Estimating population sizes for elusive animals:
559   the forest elephants of Kakum National Park, Ghana. Mol. Ecol. 12(6):1389–1402.

560 Elenga G., Bonenfant C., Péron G., 2020. Distance sampling of duikers in the rainforest:
561   Dealing with transect avoidance. PLoS One 15(10):e0240049.

562 Frantz A.C., Roper T.J., 2006. Simulations to assess the performance of different
563   rarefaction methods in estimating population size using small datasets. Conserv.
564   Genet. 7(2):315–318.

565 Gaillard J.M., Loison A., Toïgo C., 2003. Variation in life history traits and realistic
566   population models for wildlife management. In: Festa-Bianchet M., Apollonio M.
567   (Eds.) Animal Behaviour and Wildlife Conservation, Island Press, 115–132.

568 Gilbert N.A., Clare J.D., Stenglein J.L., Zuckerberg B., 2021. Abundance estimation of
569   unmarked animals based on camera-trap data. Conserv. Biol. 35(1):88–100.

570 Hamel S., Killengreen S.T., Henden J.A., Eide N.E., Roed-Eriksen L., Ims R.A., Yoccoz
571   N.G., 2013. Towards good practice guidance in using camera-traps in ecology:
572   influence of sampling design on validity of ecological inferences. Methods Ecol.
573   Evol. 4(2):105–113.

574 Hayward M.W., O'Brien J., Kerley G.I., 2007. Carrying capacity of large African
575   predators: predictions and tests. Biol. Conserv. 139(1-2):219–229.

576 Jachmann H., 2002. Comparison of aerial counts with ground counts for large african
577   herbivores. J. Appl. Ecol. 39(5):841–852.

578 Jachmann H., 2012. Estimating abundance of African wildlife: an aid to adaptive
579   management. Springer Science & Business Media.

580 Jackson R.M., Roe J.D., Wangchuk R., Hunter D.O., 2006. Estimating snow leopard
581   population abundance using photography and capture-recapture techniques. Wildl.
582   Soc. Bull. 34(3):772–781.

583 Karanth K.U., Nichols J.D., 1998. Estimation of tiger densities in India using
584   photographic captures and recaptures. Ecology 79:2852–5862.

585

586 Kéry M., Schaub M., 2011. Bayesian population analysis using WinBUGS: a hierarchical
587   perspective. Academic Press.

588 Kiffner C., Binzen G., Cunningham L., Jones M., Spruiell F., Kioko J., 2020. Wildlife
589   population trends as indicators of protected area effectiveness in northern
590   tanzania. Ecol. Indic. 110:105903.

591 Knape J., Arlt D., Barraquand F., Berg Å., Chevalier M., Pärt T., Ruete A., Zmihorski˙ M.,
592   2018. Sensitivity of binomial *N*-mixture models to overdispersion: The importance
593   of assessing model fit. Methods Ecol. Evol. 9(10):2102–2114.

594 Kohn M.H., York E.C., Kamradt D.A., Haught G., Sauvajot R.M., Wayne R.K., 1999.
595   Estimating population size by genotyping faeces. Proc. R. Soc. Lond. B Biol. Sci.
596   266(1420):657–663.

597 Kéry M., 2018. Identifiability in *N*-mixture models: A large-scale screening test with
598   bird data. Ecology 99(2):281–288.

599 Kéry M., Royle J.A., 2020. Applied Hierarchical Modeling in Ecology: Analysis of
600   distribution, abundance and species richness in R and BUGS: Volume 2: Dynamic
601   and Advanced Models. Academic Press.

602 Kéry M., Royle J.A., Plattner M., Dorazio R.M., 2009. Species richness and occupancy
603   estimation in communities subject to temporary emigration. Ecology 90(5):1279–
604   1290.

605 Le Cœur C., Thibault M., Pisanu B., Thibault S., Chapuis J.L., Baudry E., 2015.
606   Temporally fluctuating selection on a personality trait in a wild rodent population.
607   Behav. Ecol. 26(5):1285–1291.

608 Lebreton J.D., Burnham K.P., Clobert J., Anderson D.R., 1992. Modeling survival and
609   testing biological hypotheses using marked animals: a unified approach with case
610   studies. Ecol. Monogr. 62:67–118.

611 Lee D.E., Bond M.L., 2016. Precision, accuracy, and costs of survey methods for giraffe
612   *Giraffa camelopardalis*. J. Mammal. 97(3):940–948.

613 Lee D.E., Lohay G.G., Cavener D.R., Bond M.L., 2022. Using spot pattern recognition to
614   examine population biology, evolutionary ecology, sociality, and movements of
615   giraffes: a 70-year retrospective. Mamm. Biol. 1–17.

616   **26**

617 Leslie P., Davis D., 1939. An attempt to determine the absolute number of rats on a
618   given area. J. Anim. Ecol. 94–113.

619 Link W.A., Schofield M.R., Barker R.J., Sauer J.R., 2018. On the robustness of *N*-mixture
620   models. Ecology 99(7):1547–1551.

621 Martin J., Royle J.A., Mackenzie D.I., Edwards H.H., Kery M., Gardner B., 2011.
622   Accounting for non-independent detection when estimating abundance of
623   organisms with a Bayesian approach. Methods Ecol. Evol. 2(6):595–601.

624 McIntyre T., Majelantle T., Slip D., Harcourt R., 2020. Quantifying imperfect camera-
625   trap detection probabilities: implications for density modelling. Wildl. Res.
626   47(2):177–185.

627 McQualter K.N., 2018. The Ecology and Behaviour of Giraffe in Northern Botswana.
628   Ph.D. thesis, University of New South Wales, Australia.

629 Miele V., Dussert G., Spataro B., Chamaillé-Jammes S., Allainé D., Bonenfant C., 2021.
630   Revisiting animal photo-identification using deep metric learning and network
631   analysis. Methods Ecol. Evol. 12(5):863–873.

632 Morellet N., Gaillard J.M., Hewison A.J.M., Ballon P., Boscardin Y., Duncan P., Klein F.,
633   Maillard D., 2007. Indicators of ecological change: new tools for managing
634   populations of large herbivores. J. Appl. Ecol. 44:634–643.

635 Mseja G.A., Kisingo A.W., Stephan E., Martin E.H., 2020. Dry season wildlife census in
636   Mkomazi National Park, 2015. In: Durrant J., Martin E., Melubo K., Jensen R.,
637   Hadfield L., Hardin P., L W. (Eds.) Protected areas in Northern Tanzania – Local
638   communities, land use change, and management challenges, Springer, 133–143.

639 Muller Z., 2019. Rothschild's giraffe *Giraffa camelopardalis rothschildi* (Linnaeus,
640   1758) in East Africa: A review of population trends, taxonomy and conservation
641   status. Afr. J. Ecol. 57(1):20–30.

642 Nakashima Y., 2020. Potentiality and limitations of *N*-mixture and Royle-Nichols
643   models to estimate animal abundance based on noninstantaneous point surveys.
644   Popul. Ecol. 62(1):151–157.

645 Ndiweni T., Zisadza-Gandiwa P., Ncube H., Mashapa C., Gandiwa E., 2015. Vigilance
646   behavior and population density of common large herbivores in a southern African
647   savanna. J. Anim. Plant. Sci. 25(3):876–883.

648

649 O'Connell A., Karanth K., Nichols J.D., 2011. Camera traps in animal ecology. Springer
650   Japan, Tokyo.

651 O'Connor D., Stacy-Dawes J., Muneza A., Fennessy J., Gobush K., Chase M.J., Brown
652   M.B., Bracis C., Elkan P., Zaberirou A.R.M., 2019. Updated geographic range maps
653   for giraffe, *Giraffa spp.*, throughout sub-Saharan Africa, and implications of
654   changing distributions for conservation. Mammal. Rev. 49(4):285–299.

655 Ogutu J.O., Owen-Smith N., Piepho H.P., Said M.Y., 2011. Continuing wildlife
656   population declines and range contraction in the Mara region of Kenya during
657   1977–2009. J. Zool. 285(2):99–109.

658 Otis D.L., Burnham K.P., White G.C., Anderson D.R., 1978. Statistical inference from
659   capture data on closed animals populations. Wildl. Monogr. 62:1–133.

660 Pellerin M., Bessière A., Maillard D., Capron G., Gaillard J.M., Michallet J., Bonenfant
661   C., 2017. Saving time and money by using diurnal vehicle counts to monitor roe
662   deer abundance. Wildl. Biol. 2017(4).

663 Petit E., Valière N., 2006. Estimating population size with noninvasive capture-mark-
664   recapture data. Conserv. Biol. 20:1062–1073.

665 Plummer M., 2003. JAGS: A program for analysis of bayesian graphical models using
666   gibbs sampling. In: Proceedings of the 3rd international workshop on distributed
667   statistical computing, Vienna, Austria., vol. 124, 1–10.

668 Pollock K.H., 1976. Building models of capture-recapture experiments. J. R. Stat. Soc.
669   Series D Stat. 25(4):253–259.

670 Pollock K.H., 1980. Capture-recapture models: a review of current methods,
671   assumptions and experimental design .

672 Rovero F., Zimmermann F., Berzi D., Meek P., 2013. " which camera trap type and how
673   many do i need?" a review of camera features and study designs for a range of
674   wildlife research applications. Hystrix 24(2).

675 Royle J.A., 2004. *N*-mixture models for estimating population size from spatially
676   replicated counts. Biometrics 60(1):108–115.

677 Royle J.A., Karanth K.U., Gopalaswamy A.M., Kumar N.S., 2009. Bayesian inference in
678   camera trapping studies for a class of spatial capture–recapture models. Ecology
679   90(11):3233–3244.

680

681 Schwarz C., Seber G.A.F., 1999. A review of estimating animal abundance III. Stat. Sci.
682   14:427–456.

683 Seber G.A.F., 1982. The estimation of animal abundance and related parameters. C.
684   Griffin and Co. Ltd., London, 2nd edn.

685 Shorrocks B., 2016. The giraffe: biology, ecology, evolution and behaviour. John Wiley
686   & Sons.

687 Strandgaard H., 1967. Reliability of the Petersen method tested on a roe-deer
688   population. J. Wildl. Manag. 31:643–651.

689 Strandgaard H., 1972. The roe deer (*Capreolus capreolus*) population at Kälo and the
690   factors regulating its size. Dan. Rev. Game Biol. 7:1–205.

691 Stratford K.J., Stratford S.M., 2011. Fine-scale movements and use of space by spotted
692   hyaena (*Crocuta crocuta*) on Ongava Game Reserve, Namibia. Afr. J. Ecol.
693   49(3):343–352.

694 Strauss M.K.L., 2014. Ecological and anthropogenic drivers of giraffe (*Giraffa*
695   *camelopardalis tippelskirchi*) population dynamics in the Serengeti. Ph.D. thesis,
696   University of Minnesota.

697 Suraud J.P., Fennessy J., Bonnaud E., Issa A., Fritz H., Gaillard J.M., 2012. Higher than
698   expected growth rate of the endangered West African giraffe *Giraffa*
699   *camelopardalis peralta*: a successful human–wildlife cohabitation. Oryx 46(4):577–
700   583.

701 Swanson A., Kosmala M., Lintott C., Simpson R., Smith A., Packer C., 2015. Snapshot
702   Serengeti, high-frequency annotated camera trap images of 40 mammalian species
703   in an african savanna. Sci. Data 2(1):1–14.

704 Treydte A.C., Edwards P.J., Suter W., 2005. Shifts in native ungulate communities on a
705   former cattle ranch in Tanzania. Afr. J. Ecol. 43(4):302–311.

706 Trolliet F., Vermeulen C., Huynen M.C., Hambuckers A., 2014. Use of camera traps for
707   wildlife studies: a review. Biotechnol. Agron. Soc. Environ. 18(3):446–454.

708 Valeix M., Fritz H., Chamaillé-Jammes S., Bourgarel M., Murindagomo F., 2008.
709   Fluctuations in abundance of large herbivore populations: insights into the
710   influence of dry season rainfall and elephant numbers from long-term data. Anim.
711   Conserv. 11(5):391–400.

712   **29**

713 Veech J.A., Ott J.R., Troy J.R., 2016. Intrinsic heterogeneity in detection probability and
714   its effect on *N*-mixture models. Methods Ecol. Evol. 7(9):1019–1028.

715 Wearn O.R., Glover-Kapfer P., 2019. Snap happy: camera traps are an effective
716   sampling tool when compared with alternative methods. R. Soc. Open Sci.
717   6(3):181748.

718 Zett T., Stratford K.J., Weise F.J., 2022. Inter-observer variance and agreement of
719   wildlife information extracted from camera trap images. Biodivers. Conserv. 1–19.

720

Table 1 – Estimated population size ($\widehat{N}$) of giraffe (*Giraffa camelopardalis angolensis*) at Ongava Game Reserve, Namibia, in September 2016, from the monitoring of 12 waterholes for 21 days. The capture-recapture estimator modelled detection probability of animals accounting for daily variation (*t*), sex of individual (*sex*), and whether the giraffe has previously visited a waterhole the day before or not (*b*). *h* stands for the individual variation in detection probability. For the sake of comparisons, we present the average detection probabilities $\bar{p}$ *a posteriori* as the number of counted animals divided by $\widehat{N}$. For *N*-mixture models, abundance estimation used the number of uniquely identified giraffe each day at every waterhole, hence removing double counts (Poisson–binomial and β-binomial–binomial mixtures) to return population size and detection probability. Another *N*-mixture model used the raw number of giraffe counted at each waterhole instead (Poisson–Poisson *N*-mixture), which is the most common configuration in wildlife counts in Africa. In this case, the model accounts for multiple counts of the same giraffe. We report here the point estimate and associated 95% credible intervals as: $_{\text{lower limit}}$ mean $_{\text{upper limit}}$. C_v stands for the coefficient of variation of $\widehat{N}$.

Abundance estimator	$\widehat{N}$	$\bar{p}$	C_v
Capture-recapture p_t	$_{101}$ 101 $_{103}$	$_{0.99}$ 0.99 $_{1.00}$	1.0%
Capture-recapture p_{t+h}	$_{101}$ 103 $_{107}$	$_{0.94}$ 0.98 $_{1.00}$	1.7%
Capture-recapture $p_{t+sex+h}$	$_{101}$ 103 $_{108}$	$_{0.93}$ 0.98 $_{1.00}$	1.7%
Capture-recapture $p_{t+sex+b+h}$	$_{101}$ 104 $_{109}$	$_{0.92}$ 0.98 $_{1.00}$	2.1%
Capture-recapture $p_{t+sex\times b+h}$	$_{101}$ 104 $_{110}$	$_{0.92}$ 0.97 $_{1.00}$	2.2%
Spatially explicit capture-recapture	$_{103}$ 109 $_{115}$	$_{0.87}$ 0.92 $_{0.98}$	3.1%
Rarefaction curve (Kohn)	$_{145}$ 175 $_{215}$	$_{0.47}$ 0.57 $_{0.70}$	10.0%
Rarefaction curve (Eggert)	$_{104}$ 117 $_{134}$	$_{0.75}$ 0.86 $_{0.97}$	6.3%
N-mixture (Poisson–binomial)	$_{173}$ 215 $_{263}$	$_{0.38}$ 0.47 $_{0.58}$	4.4%
N-mixture (ZIP–binomial)	$_{173}$ 215 $_{263}$	$_{0.38}$ 0.47 $_{0.58}$	4.4%
N-mixture (β-binomial–binomial)	$_{107}$ 124 $_{156}$	$_{0.65}$ 0.81 $_{0.94}$	10.1%
N-mixture (Poisson–Poisson)	$_{79}$ 87 $_{99}$	$_{1.02}$ 1.16 $_{1.28}$[a]	5.4%

[a]For this *N*-mixture model, detection is no longer a probability but a rate that can take values > 1.

Table 2 – Reported densities of giraffe (*Giraffa camelopardalis ssp.*) populations in Africa (in number of individuals per km²). When abundance was estimated for several years, repeated lines in the same location give the range of densities recorded on the site.

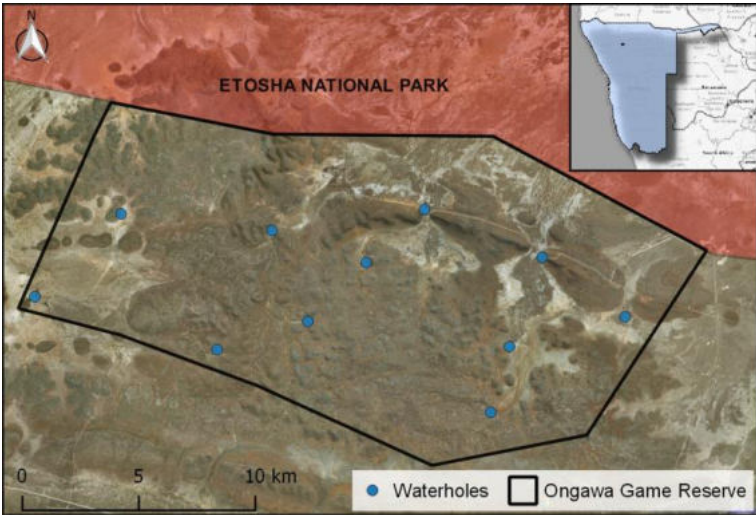| Site	Ecosystem	Country	Density	Estimator	Reference
Chobe National Park	Floodplains — mixed woodland	Botswana	0.110 (—)	Aerial counts	Mcqualter (2018)
Great Rift Valley	Savannah	Kenya	0.468 (88/188)	Ground census	Muller (2019)
Great Rift Valley	Savannah	Kenya	0.405 (77/190)	Ground census	Muller (2019)
Mara Region	Open grassland	Kenya	0.750 (—)	Aerial counts	Ogutu et al. (2011)
Mara Region	Open grassland	Kenya	0.080(—)	Aerial counts	Ogutu et al. (2011)
Etosha National Park	Savannah plains / mixed savannah	Namibia	0.150(—)	Aerial counts	Brand (2007)
Etosha National Park	Savannah plains / mixed savannah	Namibia	0.200(—)	Aerial counts	Brand (2007)
Ongava	Forest savannah	Namibia	0.336 (—)	Capture-recapture	This study
Kouré and Fandou Plateaus	Forest savannah	Niger	0.241 (—)	Census (photo ID)	Suraud et al. (2012)
Lake Manyara National Park	Evergreen groundwater forests	Tanzania	0.570 (0.570-0.580)	Distance sampling	Kiffner et al. (2020)
Lake Manyara National Park	Evergreen groundwater forests	Tanzania	1.210 (1.180-1.25)	Distance sampling	Kiffner et al. (2020)
Mkomazi National Park	Savannah-woodland ecosystem	Tanzania	1.165 (0.808)	Distance sampling	Mseja et al. (2020)
Tarangire Ecosystem	Savannah-woodland ecosystem	Tanzania	0.791 (0.073)	Capture-recapture	Lee & Bond (2016)
Tarangire Ecosystem	Savannah-woodland ecosystem	Tanzania	1.202 (0.760)	Capture-recapture	Lee & Bond (2016)
Tarangire Ecosystem	Savannah-woodland ecosystem	Tanzania	0.173 (0.057)	Capture-recapture	Lee & Bond (2016)
Saadani National Park	Savannah-forest mosaic	Tanzania	0.106—1.400	Distance sampling	Treydte et al. (2005)
Serengeti	Scrub thicket-open grassland	Tanzania	0.18—2.59	Aerial counts	Strauss (2014)
Shamwari ecosystems	Forest (?)	South Africa	0.744 (—)	Walked transects	Hayward et al. (2007)
Lupande	Mopane/miombo woodlands	Zambia	1.274 (930/730)	Double counts (aerial)	Jachmann (2002)
Hwange National Park	Forest savannah	Zimbabwe	0.170 (—)	Distance sampling	Valeix et al. (2008)
Gonarezhou National Park	Dry deciduous savannah	Zimbabwe	0.470 (0.140)	Distance sampling	Ndiweni et al. (2015)
Malipati Sarafi Area	Dry deciduous savannah	Zimbabwe	0.010 (0.030)	Distance sampling	Ndiweni et al. (2015)

784 **Figure legend**

785 **Figure 1** – Spatial distribution of waterholes surveyed in 2016 with camera traps to
786 monitor wildlife abundance at Ongava Game Reserve, Namibia. We extracted
787 abundance data for giraffe (*Giraffa camelopardalis angolensis*) to be apply to
788 different estimators of giraffe population size.

789 **Figure 2** – Rarefaction curves for individual giraffe (*Giraffa camelopardalis*
790 *angolensis*) detected during the 21-day study period on Ongava Game Reserve,
791 Namibia (step curve in black). Continuous lines and associated shaded areas
792 represent predictions and credible intervals of rarefaction models. We fitted two
793 rarefaction equations proposed by Eggert et al. (2003) and Kohn et al. (1999) to
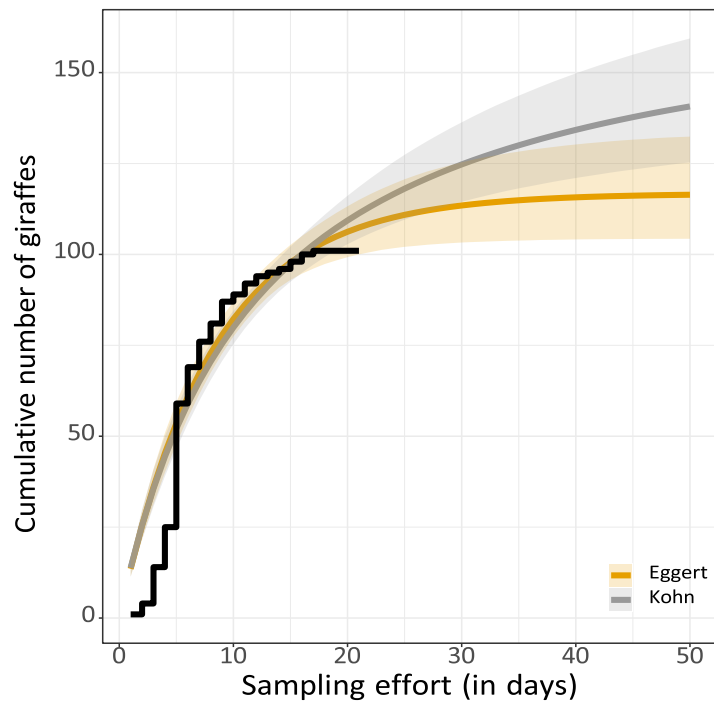794 the problem of population size estimation using a Bayesian framework.

795

796

797

Figure 1 –

799

Figure 2 –